Pergamon

Bioorganic & Medicinal Chemistry, Vol. 5, No. 1, pp 49–64, 1997

PII: S0968-0896(96)00212-X
0968-0896/97 $17.00 + 0.00

Regulation of Stress-Induced Cytokine Production by Pyridinylimidazoles; Inhibition of CSBP Kinase

Timothy F. Gallagher,*[a] George L. Seibel,[b] Shouki Kassis,[c] Jeffrey T. Laydon,[c] Mary Jane Blumenthal,[c] John C. Lee,[c] Dennis Lee,[a] Jeffrey C. Boehm,[a] Susan M. Fier-Thompson,[a] Jeffrey W. Abt,[a] Margaret E. Soreson,[a] Juanita M. Smietana,[a] Ralph F. Hall,[a] Ravi S. Garigipati,[a] Paul E. Bender,[a] Karl F. Erhard,[a] Arnold J. Krog,[a] Glenn A. Hofmann,[d] Peter L. Sheldrake,[e] Peter C. McDonnell,[f] Sanjay Kumar,[f] Peter R. Young[f] and Jerry L. Adams[a]

Departments of [a]Medicinal Chemistry, [b]Physical & Structural Chemistry, [c]Cellular Biochemistry, [d]Biomolecular Discovery, [e]Chemical Development and [f]Molecular Immunology, SmithKline Beecham Pharmaceuticals, King of Prussia, PA 19406-0939, USA

Abstract.—Members of three classes of pyridinylimidazoles bind with varying affinities to CSBP (p38) kinase which is a member of a stress-induced signal transduction pathway. Based upon SAR and protein homology modeling, the pharmacophore and three potential modes of binding to the enzyme are presented. For a subset of pyridinylimidazoles, binding is shown to correlate with inhibition of CSBP kinase activity, whereas no significant inhibition of PKA, PKCα and ERK kinase activity is observed.

Introduction

Intracellular signal transduction is the means by which cells respond to extracellular stimuli. Regardless of the nature of the cell surface receptor (e.g. protein tyrosine kinase of seven-transmembrane G-protein coupled), protein kinases and phosphatases along with phospholipases are the essential machinery by which the signal is further transmitted within the cell.[1] Protein kinases can be categorized into five classes with the two major classes being, tyrosine kinases and serine/threonine kinases depending upon whether the enzyme phosphorylates its substrate(s) on specific tyrosine(s) or serine/threonine(s) residues.[2]

For most biological responses, multiple intracellular kinases are involved and an individual kinase can be involved in more than one signaling event. These kinases are often cytosolic and can translocate to the nucleus or the ribosomes where they can affect transcriptional and translation events, respectively. The involvement of kinases in transcriptional control is presently much better understood than their effect on translation as illustrated by the studies on growth factor induced signal transduction involving MAP kinase (ERK).[3]

While many signaling pathways are part of cell homeostasis, numerous cytokines (e.g. IL-1 and TNF) and certain other mediators of inflammation (e.g. COX-2) are produced only as a response to stress such as bacterial lipopolysaccharide (LPS). The first indications suggesting that the signal transduction pathway leading to LPS induced cytokine biosynthesis involved protein kinases came from studies of Weinstein et al.,[4] but the specific protein kinases involved were not identified. Furthermore, the fact that these mediators are produced in large quantities only in response to stress led these investigators to suggest that their synthesis may involve an independent signal transduction pathway(s). Working from a similar perspective, Han et al.[5] identified murine P38 as a kinase which is tyrosine phosphorylated in response to LPS.

Our involvement in protein kinases and signal transduction evolved from a different perspective. While we had a general interest in LPS-induced cytokine production, we were specifically interested in elucidating the mechanism of action of a class of pyridinylimidazole anti-inflammatory compounds for which SK&F 86002 (**I**) was the prototypic example. These compounds, in addition to their effects on eicosanoid production, consistently inhibited IL-1 and TNF synthesis in human monocytes at concentrations in the low μM range[6] and exhibited activity in animal models which are refractory to NSAIDs (non-steroidal anti-inflammatory drugs).[7] The ability of these molecules to suppress cytokine production prompted their designation as CSAID™ compounds.

In order to understand the mechanism of action of the pyrinylimidazoles, we took several approaches. Biochemical studies found that the predominant effect of these compounds on TNF biosynthesis occurs at the protein level and little effect was seen at the level of transcription.[8,9] A series of 2,4,5-triarylimidazoles was

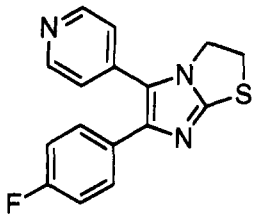

SK&F 86002 (I)

IL-1 inhibition IC_{50} = 0.50 μM

CSBP binding IC_{50} = 0.26 μM

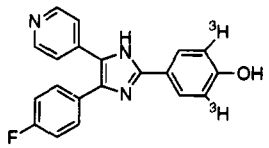

SB 202190 (II)

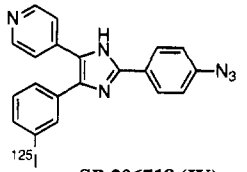

SB 206718 (IV)

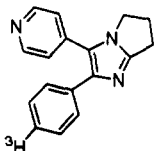

SK&F 108965 (III)

prepared to investigate the SAR (structure–activity relationships) of cytokine inhibition. The results from this study demonstrated that cytokine inhibition was not related to 5-lipoxygenase inhibition nor the nonspecific antioxidant properties of these compounds.[10] Furthermore, in the course of preparing the 2,4,5-triarylimidazoles several compounds were discovered to be more potent inhibitors of cytokine production (~50 nM range) than any inhibitors previously identified. The discovery of these potent inhibitors was a crucial factor leading to the identification of the molecular target for the pyridinylimidazoles. Radiolabeling one of these inhibitors (**II**) enabled the development of a competitive binding assay which was used to demonstrate high affinity binding to a single site of low abundance (~5 pmol/mg). The usefulness of this assay was in contrast to an earlier attempt to configure an assay based on a less potent radiolabeled pyrroloimidazole (**III**, IC_{50} = 0.50 μM for IL-1 inhibition). Further SAR studies led to the preparation of a radioaffinity label (**IV**) with submicromolar binding affinity. This compound served as a key tool in the purification, sequencing, cloning, expression and characterization of the target protein. The molecular targets were identified as a pair of closely related novel serine/threonine protein kinases of the MAP kinase family and structurally homologous to HOG-1, a MAP kinase which restores the osmotic gradient across the cell membrane of *Saccharomyces cerevisiae* in response to the stress of increased extracellular salt concentration.[11] These kinases were termed CSAID™ binding proteins 1 and 2 (CSBP1, CSBP2).[12] CSBP2 differs by only two amino acids from murine P38[5] kinase and is identical to human P38.[13]

It is now firmly established that CSBP is one of several kinases that are involved in a stress–response signal transduction pathway. Stress signals, including LPS and pro-inflammatory cytokines, activate MKK 3/4 and 6[14–17] upstream from CSBP which in turn phosphorylate CSBP at threonine 180 and tyrosine 182 resulting in CSBP activation. MAPKAP kinase-2[18] and MAPKAP kinase-3[19] have been identified as downstream substrates of CSBP which in turn phosphorylate heat shock protein Hsp 27 (Fig. 1). It is not yet known whether MAPKAP-2, MAPKAP-3 or HSP-27 are involved in cytokine biosynthesis.

What is known, however, is that the pyrimidinylimidazoles affect the synthesis of TNF,[8,9] IL-1[20] and other pro-inflammatory proteins whose mRNAs contain AU rich motifs in their 3′ UTR region[21] through the regulation of protein translation. Therefore, it is conceivable that CSBP or a downstream kinase in this pathway phosphorylates a protein or a protein complex bound to the AUUUA regions of the cytokine mRNA resulting in release of translational repression allowing protein synthesis to occur (Fig. 1). The phenomenon of release of translational repression was originally proposed by Beutler et al.[22] for the proinflammatory cytokine TNF as a secondary switch to protect against its overproduction under normal circumstances given the powerful and often destructive effects that TNF exerts. This group demonstrated that in CAT reporter gene constructs in which various substitution/deletions in the 5′- and 3′-UTR regions of TNF mRNA were made and transfected into macrophage and nonmacrophage cell lines, that deletion of an AUUUA repeated motif in the 3′-UTR of the TNF mRNA led to constitutive synthesis in vitro and in transgenic animals. In similar reporter constructs, CSAID™ compounds have been shown to inhibit CAT expression.[23] These studies provide strong evidence that the mRNA of pro-inflammatory cytokines may exist in sufficient levels at all times, but is largely in a repressed state with translation occurring only when the cell is insulted by a number of stresses. Inhibition of the kinases required for translational derepression, therefore, may inhibit the bursts of cytokine production that are associated with disease[24] and not the cytokine levels required for normal cell function. Consequently, selective inhibition of CSBP (or another kinase along this pathway) provides an attractive target for drug development.

Previously, we reported that a series of 2,4,5-triarylimidazoles inhibited IL-1 production in human macrophages.[10] We show here that this inhibition is the result of binding to CSBP and subsequent inhibition of kinase activity which leads to the regulation of cytokine biosynthesis. One of these inhibitors (SB 203580, **7**) was shown to be highly selective versus 14 different kinases and phosphatases.[18] Kinase selectivity data for additional members of this class is provided for CSBP versus MAP kinase, PKA and PKCα. Based upon

structure activity relationships within this class of compounds and those observed in other classes of pyridinylimidazoles, the proposed pharmacophore for pyridinylimidazole binding is presented. Three binding modes of SB 203580 to a CSBP homology model are proposed which accommodate the SAR presented herein.

Results and Discussion

Biological studies

Table 1 lists the IC_{50}s of 13 2,4,5-triarylimidazoles for CSBP binding, CSBP, ERK, PKA and PKCα kinase inhibition. Figure 2 shows that an excellent correlation exists between CSBP binding and inhibition of CSBP kinase activity. The data in Table 1 comparing kinase activities clearly shows that the selectivity previously observed for **7** is a general property of this structural class. In addition to the compounds presented in Table 1, the IC_{50}s for CSBP binding and inhibition of IL-1 biosynthesis[25] of structurally diverse members of three classes of pyridinylimidazoles are shown in Tables 2–6. In general, binding values parallel those obtained in the whole cell assays.[26] Therefore, the binding data presented in these tables forms the basis for the following discussions on the SAR of cytokine inhibition and the construction of the pyridinylimidazole pharmacophore.

Chemistry

All the 2,4,5 triarylimidazoles were prepared according to either route **A** or route **B**[10] as depicted in Scheme 1. The 4,5-diaryl-*N*-1 substituted imidazoles were prepared as shown in Scheme 2. The 2,3-diarylpyrrolo-imidazole derivatives were prepared as illustrated in Scheme 3. The synthesis of SK&F 86002 (**I**) has been described elsewhere.[27]

SAR/pharmacophore requirements

Inspection of the binding data in Table 2 illustrates the minimal requirements for activity in all three series of pyridinylimidazoles.[28] In the 2,4,5 triaryimidazole

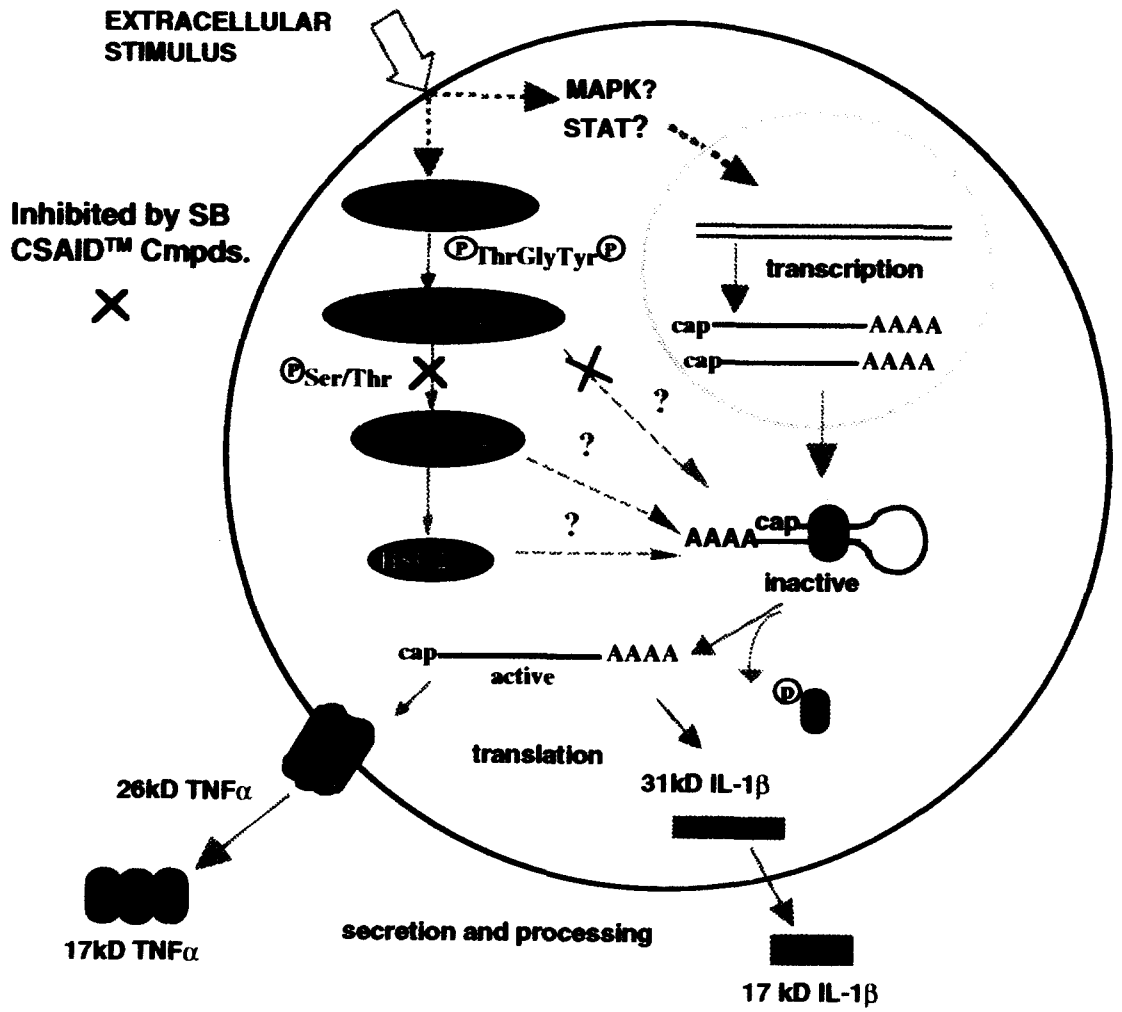

Figure 1. Proposed model for the role of CSBP in a novel kinase signalling pathway and subsequent regulation of extracellular-induced cytokine biosynthesis in human monocytes. Upon stimulation by LPS both IL-1 and TNF transcription and translation increase. Active translation of proteins having a 3′-AU rich mRNA requires a CSBP directed phosphorylation of the translational complex to release translational repression.

series, the lack of binding activity of the 4,5-diphenyl analogue (**1**) versus the corresponding 4-pyridyl compound (**2**) shows the importance of the pyridine ring. In the 4,5-diaryl-*N*-1 substituted series the lack of activity of the 2- and 3-pyridinyl derivatives (**3** and **4**, respectively) versus the corresponding 4-pyridyl derivative (**5**), not only reinforces the crucial role of the pyridine ring, but also demonstrates the importance of the position of the pyridine nitrogen within the ring for activity. In the 2,4,5-triarylimidazole series, the inactivity demonstrated for the ethyl analogue (**6**) compared with a 4-fluorophenyl derivative (e.g. **7**) illustrates the need for a second aromatic ring adjacent to the 4-pyridyl group. Likewise, in the pyrroloimidazole series, the inactivity of the chloro analogue (**8**) compared with the corresponding 4-fluorophenyl derivative (**9**) demonstrates the need for this second aromatic ring. The activities of the 2-thiophenyl (**10**), and the 1- and 2-naphthyl analogues (**11** and **12**, respectively) compared with **7** illustrate that aromatic groups other than phenyl are tolerated. A large decrease in binding affinity, however, is observed with the 1 and 2-naphthyl compounds (~50- and 100-fold for **11** and **12**, respectively) due most likely to steric factors (see Table 4). The dramatic differences observed for regioisomers (**9** versus **13** and **14** versus **15**) reveals that the imidazole nitrogen β to the

Table 1. Kinase activity [(IC_{50}s (μM)]

No.	CSBP		ERK	PKA	PKCα
	Binding	Kinase			
1	>10	>2.5	>10	>100	>100
2	0.080	0.089	>10	>100	>100
6	>30	>2.5	>10	>100	>100
7	0.042	0.074	>10	>100	>100
39	3.9	7.5	>10	>100	>100
40	0.15	0.21	>10	>100	7.6
42	0.66	0.91	>10	>100	>100
43	0.34	0.18	>10	>100	>100
47	0.23	0.17	>10	>100	>100
49	0.085	0.083	>10	>100	38
51	0.0030	0.0012	>10	>100	38
55	0.050	0.067	>10	>100	>100
61	>30	>2.5	>10	>100	>100

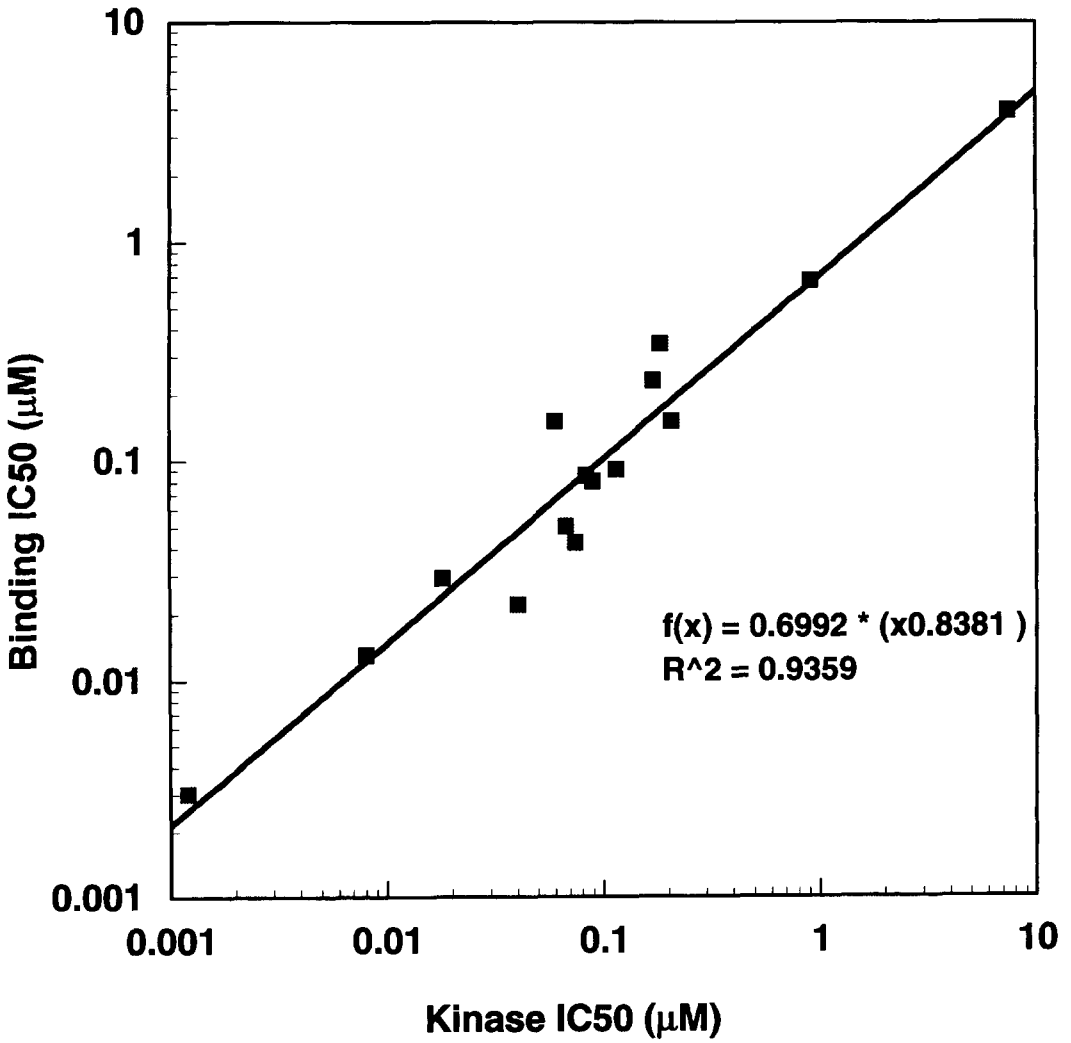

Figure 2. Potency of CSAID™ compounds in CSBP binding and kinase activity. CSBP kinase activity and competition binding were determined as in the Experimental. Data represent most of the compounds listed in Tables 1 and 4 additional CSAID™ compounds from different chemical classes. The IC_{50} values were calculated from % inhibition data obtained using serial dilutions of compounds..

Table 2. Pyridinylimidazoles—minimum binding requirements

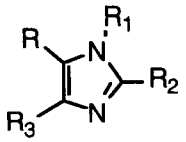

No.	R	R_1	R_2	R_3	IL-1 monocytes IC_{50} (μM)	CSBP binding IC_{50} (μM)
1	Ph	H	4-NO_2Ph	4-FPh	>5	>10
2	4-Pyridyl	H	4-NO_2Ph	4-FPh	0.05	<0.1
3	2-Pyridyl	3-Morpholinopropyl	H	4-FPh	—	>10
4	3-Pyridyl	3-Morpholinopropyl	H	4-FPh	—	>10
5	4-Pyridyl	3-Morpholinopropyl	H	4-FPh	0.60	0.12
6	4-Pyridyl	H		Et	>5	>30
7	4-Pyridyl	H	4-S(O)MePh	4-FPh	0.08	0.042
8	4-Pyridyl	—$(CH_2)_3$—		Cl	—	>50
9	4-Pyridyl	—$(CH_2)_3$—		4-FPh	0.17	0.066
10	4-Pyridyl	H	4-S(O)MePh	2-Thiophenyl	—	0.46
11	4-Pyridyl	H	4-S(O)MePh	1-Naphthyl	0.65	2.3
12	4-Pyridyl	H	4-A(O)MePh	2-Naphthyl	0.77	5.6
13	4-FPh	—$(CH_2)_3$—		4-Pyridyl	—	>10
14	4-Pyridyl	—$(CH_2)_2$OAc	H	4-FPh	—	0.050
15	4-FPh	H	—$(CH_2)_2$OAc	4-Pyridyl	—	>10

4-pyridyl ring must be unhindered to enable the pyridinylimidazoles to bind to CSBP.

Table 3 shows the result of adding substituents to the pyridine ring. In the 2,4,5-triarylimidazole series, placement of a methyl group at the 2-position and substitution of the pyridine with quinoline lead to approximately 10-fold decreases in binding (**16** and **17**, respectively, versus **7**). In the N-1 substituted series, the same substitutions lead to approximately 25- and 75-fold decreases in binding (**18** and **19**, respectively, versus **5**) affinity. 2,6-Dimethyl-substitution (**20**) further reduces binding affinity.

Results in Table 4 suggest a similar pattern for all three series regarding substitution on the aryl ring adjacent to the pyridine. In the pyrroloimidazole series, only the 3- and 4-chlorophenyl analogues (**21** and **22**, respectively) exhibit potency comparable to the 4-fluorophenyl derivative (**9**). Substitution of chlorine at the 2-position (**23**) leads to a modest decrease in activity. Substituents larger than chlorine at the 4-position lead to diminished binding affinity (compare the Br, OMe, SMe and SEt analogues **24**, **25**, **26** and **27**, respectively, versus **9**). Polar substituents at this position eliminate the ability of the compounds to bind to the enzyme [compare the S(O)Me, and SO_2Me

Table 3. Pyridine replacements

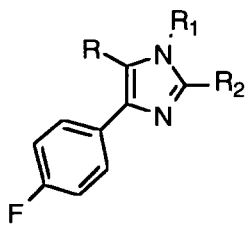

No.	R	R_1	R_2	IL-1 monocytes IC_{50} (μM)	CSBP binding IC_{50} (μM)
7	4-Pyridyl	H	4-S(O)MePh	0.08	0.042
16	2-Me-4-pyridyl	H	4-S(O)MePh	0.43	0.37
17	4-Quinolyl	H	4-S(O)MePh	0.71	0.44
5	4-Pyridyl	3-Morpholinopropyl	H	0.60	0.12
18	2-Me-4-pyridyl	3-Morpholinopropyl	H	—	3.0
19	4-Quinolyl	3-Morpholinopropyl	H	—	9.0
20	2,6-Di-Me-4-pyridyl	3-Morpholinopropyl	H	—	25

analogues **28** and **29**, respectively to **26**]. In the N-1 substituted series, as in the pyrroloimidazole series, the 3-chlorophenyl analogue (**30**) binds with affinity comparable to the 4-fluorophenyl derivative (**5**). In this series, a direct comparison between analogues which possess a bulky substituent at the 3- and 4-positions was made. The 3- and 4-trifluoromethyl derivatives (**31** and **32**, respectively) show that this group is much better tolerated at the 3-position compared with the 4-position. Similarly, the 3-methylthio analogue (**33**) in this series binds only 2.5 times weaker than **5**. In contrast to the steric tolerance seen for mono-substitution at the *meta*-position, the 3,5-bis-trifluoromethyl analogue (**34**) exhibits almost a 1000-fold decrease in binding. Introduction of the polar sulfoxide substituent at the 3-position (**35**) leads to approximately a 40-fold decrease in binding affinity compared with **5**. In the 2,4,5-triarylimidazole series, only compounds substituted at C-2 and C-3 of the phenyl ring (with the exception of the naphthyl derivatives **11** and **12**) were prepared. As in the other two series, the 3-chlorophenyl analogue (**36**) binds with affinity comparable to the 4-fluorophenyl derivative (**7**). The 3-OMe (**37**) and the 2-OMe (**38**) analogues show decreases in binding of approximately 10- and 100-fold, respectively, compared with **7**. As in the other two series, placement of a polar functionality on this phenyl ring (**39**) leads to a large decrease in binding affinity (~100-fold compared with **7**.

A wide variety of substituents are tolerated at the 1- and 2-positions of the imidazole. There are functionalities, however, which can either enhance or diminish activity and their effects can differ depending upon whether they are placed at N-1 or C-2. In the 2,4,5-triarylimidazole series, the compound with an unsubstituted phenyl ring (**40**) binds to CSBP with an IC_{50} of 0.15 μM. In order to assess the effect of placing substituents at the *ortho*-, *meta*- and *para*-positions around this ring, the corresponding sulfide (**41**, **42** and **43**, respectively), sulfoxide (**44**, **45** and **7**, respectively) and sulfone analogues (**46**, **47** and **48**, respectively) were prepared. Analysis of the data (Table 5) clearly shows that only placement of the polar sulfoxide and sulfone functionalities at the 4-position (**7** and **48**) leads to enhanced binding. This enhancement in binding also occurs with other polar substituents at the 4-position regardless of whether they are neutral (**49** and **50**), basic (**51**, **52**, **53** and **54**) or weakly acidic (**55**, **56** and **57**). The highly acidic 4-carboxyl derivative **58**, which exists as the carboxylate anion at pH 7, does not lead to enhanced activity. Again, comparison of the 4-OH (**55**) and the 2-OH (**59**) analogues illustrates that the increase in binding affinity occurs only when a

Table 4. Phenyl substitution

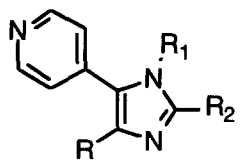

No.	R	R_1	R_2	IL-1 monocytes IC_{50} (μM)	CSBP binding IC_{50} (μM)
9	4-FPh	$-(CH_2)_3-$		0.17	0.066
21	3-ClPh	$-(CH_2)_3-$		0.050	0.040
22	4-ClPh	$-(CH_2)_3-$		—	0.050
23	2-ClPh	$-(CH_2)_3-$		—	0.25
24	4-BrPh	$-(CH_2)_3-$		0.70	3.2
25	4-MeOPh	$-(CH_2)_3-$		4.2	3.6
26	4-MeSPh	$-(CH_2)_3-$		2.7	3.4
27	4-EtSPh	$-(CH_2)_3-$		>20	5.6
28	4-MeS(O)Ph	$-(CH_2)_3-$		>10	>10
29	4-$MeSO_2$Ph	$-(CH_2)_3-$		>10	>10
5	4-FPh	3-Morpholinopropyl	H	0.60	0.12
30	3-ClPh	3-Morpholinopropyl	H	—	0.21
31	3-CF_3Ph	3-Morpholinopropyl	H	—	0.46
32	4-CF_3Ph	3-Morpholinopropyl	H	—	3.0
33	3-MeSPh	3-Morpholinopropyl	H	1.0	0.29
34	3,5-Di-CF_3Ph	3-Morpholinopropyl	H	—	114
35	3-MeS(O)Ph	3-Morpholinopropyl	H	>5	5.0
7	4-FPh	H	4-MeS(O)Ph	0.08	0.042
36	3-ClPh	H	4-MeS(O)Ph	0.08	0.030
37	3-MeOPh	H	4-MeS(O)Ph	0.59	0.38
38	2-MeOPh	H	4-MeS(O)Ph	1.14	3.3
39	3-$MeSO_2NHPh$	H	4-MeS(O)Ph	>5	3.9

polar group is placed at the 4-position. Comparison of the activities of the *N,N*-dimethylamino compounds **52** and **60** demonstrates that for enhanced activity, the polar functionality cannot be too far removed from the 4-position of the 2-phenyl ring. The activity observed with **56**, **57** and **60** show that placement of large groups at the 4-position are tolerated, however, the lack of activity observed for the 3,5-di-*tert*-butylphenol derivative (**61**) indicates that steric tolerance at C-2 is not unlimited.

Table 6 shows that sterically demanding groups (**62** versus **5** and **63–70**) are well tolerated at N-1 and that highly lipophilic substituents (e.g. **63**, **64** and **65**) lead to enhanced potency. Basic substituents (**5** and **66**) are well tolerated but do not appear to affect binding affinity to any significant degree. Polar functionalities are well tolerated at N-1 (e.g. **67**, **68** and **70**), except in the case of the carboxypropyl moiety (**71**), which most likely exists as the carboxylate anion at pH 7 and decreases binding affinity by over an order of magnitude.

The data presented in Tables 3 and 4 show that while a given substituent on the pyridine or the adjacent phenyl ring can exert different effects on the magnitude of binding among the three classes of pyridinylimidazoles, trends are the same among the classes. If placed in the context of the minimal structural requirements (Table 2) needed for binding by all the pyridinylimidazoles, the data suggest that the same pharmacophore exists for all three classes. Consequently, we believe that the small differences observed for a given substituent among the three series result either from the differential effects that the substituent exerts on the conformation of the inhibitor or from minor changes in the fit of compounds from the three different series of pyrindinylimidazoles within the enzyme binding pocket. The SAR does not suggest radically different binding modes for the three series. Figure 3 summarizes the above SAR observations and illustrates the pyridinylimidazole pharmacophore.

Table 5. 2-Phenyl substituted 2,4,5-triarylimidazoles

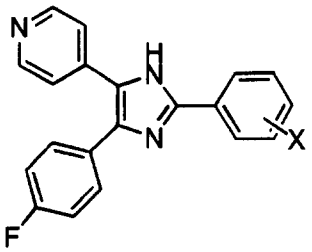

No.	X	IL-1 inhibition monocytes IC_{50} (μM)	CSBP binding IC_{50} (μM)
40	H	0.30	0.15
41	2-SCH_3	0.82	0.35
42	3-SCH_3	0.93	0.66
43	4-SCH_3	0.58	0.34
44	2-$S(O)CH_3$	0.71	0.58
45	3-$S(O)CH_3$	0.70	0.20
7	4-$S(O)CH_3$	0.08	0.042
46	2-SO_2CH_3	0.74	0.23
47	3-SO_2CH_3	0.62	0.23
48	4-SO_2CH_3	0.20	0.030
49	4-SO_2NH_2	0.05	0.085
50	4-NH-SO_2CH_3	0.27	0.06
51	4-CH_2NH_2	0.05	0.003
52	4-$CH_2N(CH_3)_2$	0.08	0.06
53	4-NH_2	0.05	<0.10
54	4-$N(CH_3)_2$	0.35	0.08
55	4-OH	0.05	0.050
56	4-$CH_2N(OH)C(O)NH_2$	0.20	0.024
57	4-(Oxadiazol-5-one-3-yl)	0.86	0.03
58	4-CO_2H	0.50	0.49
59	2-OH	3.0	3.9
60	4-$O(CH_2)_3N(CH_3)_2$	0.29	0.44
61	3,5-Di-*tet*-butyl,5-OH	>5	>30

Table 6. N-1 substituted 4,5-diarylimidazoles

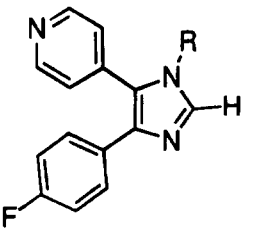

No.	X	IL-1 inhibition monocytes IC_{50} (μM)	CSBP binding IC_{50} (μM)
62	H	—	0.21
63	3-Benzylaminopropyl	0.59	0.07
64	3-Phenoxypropyl	—	0.07
65	3-Phenylthiopropyl	—	0.08
5	3-Morpholinopropyl	0.60	0.12
66	1-Benzylpiperdin-4-yl	—	0.44
67	3-Phenylsulfinylpropyl	—	0.63
68	3-Carbomethoxypropyl	—	0.29
69	4-Methylthiophenyl	—	1.5
70	4-Methylsulfinylphenyl	2.3	0.75
71	3-Carboxypropyl	—	3.8

Molecular modeling studies

In order to gain insight into the manner in which the pyridinylimidazoles bind to CSBP and assist in the design of more potent and selective inhibitors, a homology model of CSBP was constructed. The model was based on the X-ray crystal structure for ERK[29] since this enzyme shows the greatest homology to CSBP among kinases for which X-ray crystal data is available. The X-ray structure determined for ERK is an open and unphosphorylated form. The homology model necessarily represents a similar state of CSBP. Using myelin basic protein as the substrate, several CSAID™ compounds have been shown to be competitive inhibitors with respect to ATP and, therefore, most likely compete with ATP in the ATP binding pocket.[30] The pyridinylimidazoles have also been shown to bind to both the unphosphorylated (unactivated) and the phosphorylated (activated) forms of the enzyme.[31]

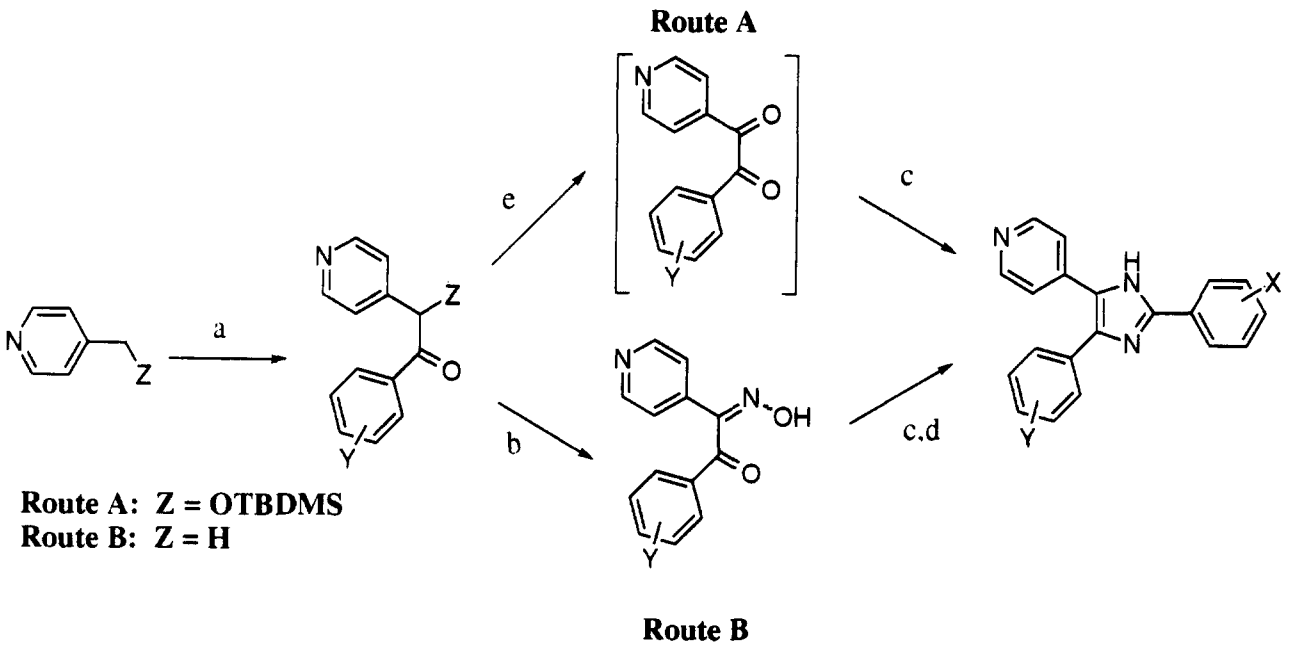

Scheme 1. Synthesis of 2,4,5-triarylimidazoles. (a) LDA, THF, Y-Ph(CO)N(OMe)Me; (b) $NaNO_2$, HCl, H_2O; (c) X-PhCHO, NH_4OAc; (d) $P(OMe)_3$; (e) $Cu(OAc)_2$.

Unactivated PKA exists in a relatively open conformation with respect to the ATP-binding site, however, upon phosphorylation, the enzyme undergoes a conformational change and as a result can interconvert between the open and closed forms.[32] Since the pyridinylimidazoles have been shown to bind to the phosphorylated (activated) form of CSBP, it is conceivable, by analogy with PKA, that these compounds may bind to either the open, closed or perhaps an intermediate form of the activated enzyme. Since these inhibitors have also been shown to bind to the unactivated form (open by analogy with PKA) of CSBP, we initiated studies docking the pyridinylimidazoles into the CSBP homology model based on the unactivated (open) ERK structure.

Since we feel that the pyridinylimidazoles are represented by a single pharmacophore, we have attempted to develop binding hypotheses which are consistent wih the SAR for all three classes of pyridinylimidazoles. Our strategy for finding possible binding modes for the pyridinylimidazoles consisted of the following: (1) for a

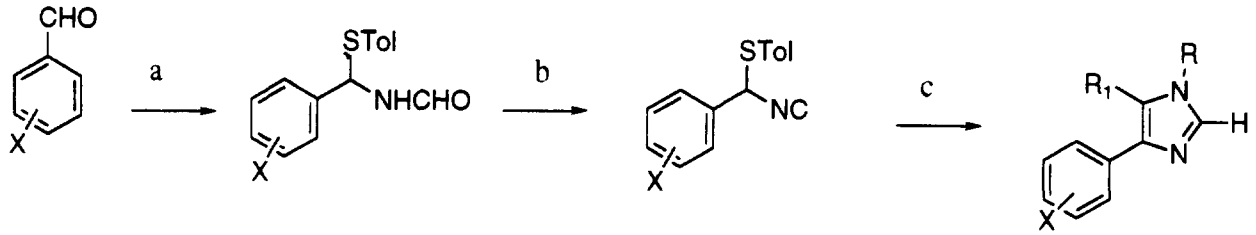

Scheme 2. Synthesis of N-1-alkyl-4,5-diarylimidazoles: (a) TolSH, $NCONH_2$; (b) $POCl_3$; (c) R_1=NR, TBD.

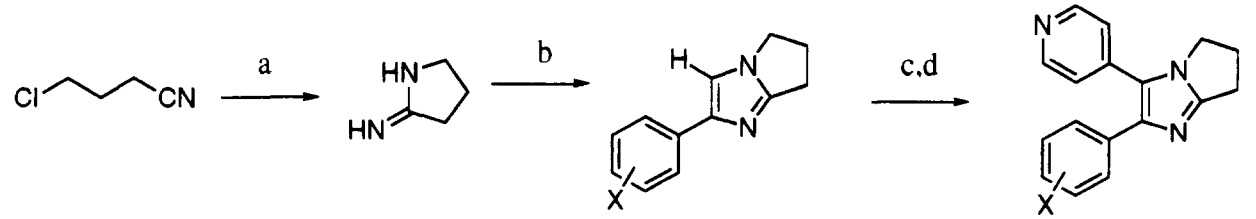

Scheme 3. Synthesis of 2,3-diarylpyrroloimidazoles: (a) NH_3, $NaOCH_3$; (b) X-PhC(O)CH_2Cl; (c) C_5H_5N, EtOC(O)Cl; (d) *tert*-BuOK, *tert*-BuOH.

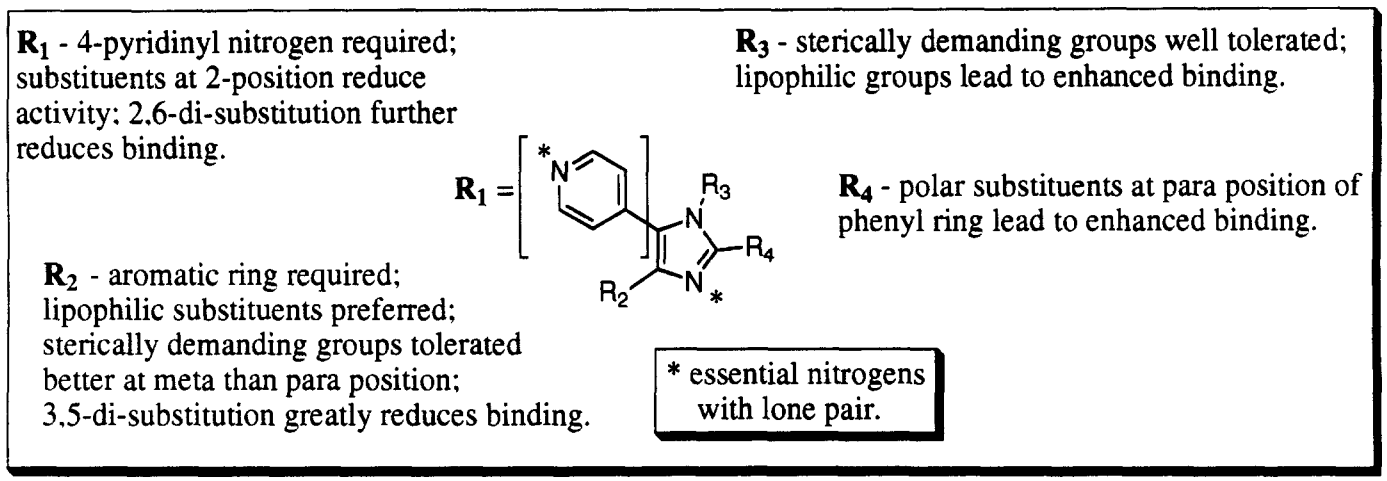

Figure 3. CSBP binding pharmacophore for pyridinylimidazoles.

given pyridinylimidazole, low-energy conformations were generated using MacroModel (see experimental). (2) Each conformer of the inhibitor was docked into the ATP binding pocket of the kinase using DOCK 3.5 with scores based on VDW complementarity between ligand and protein. (3) The highest scoring binding orientations were manually screened by assessing their abilities to accommodate the existing SAR. (4) Final minor adjustments to the binding modes were carried out by hand. Since the protein structure was a homology model, and the exact positionings of the amino acid sidechains were unknown, a maximum of two closer than VDW contacts during the DOCK search were allowed.

Figure 4(a) shows ATP bound in the CSBP homology model (positioned as in ERK) while Figures 4(b)–(d) display three possible binding modes of SB 203580. The wedge shape of the 1,2-diarylimidazole moiety permits one the aromatic rings to interact with the top lobe and the other aromatic ring to interact with the bottom lobe of the ATP pocket [Figs 4(b) and (c)]. In addition, both orientations accommodate substituents on the imidazole N-1 position, a feature observed for several potent inhibitors (see SAR discussion). Figure 4(d) shows a binding mode in which both aryl rings make extensive VDW contacts with the top lobe of the ATP binding pocket and in which the inhibitor is bound more deeply within the pocket than those proposed in Figures 4(b) and (c). All three dockings are consistent with the following aspects of the SAR: (1) There are no steric impediments to substitution at the imidazole N-1 position. (2) There are limitations to the size of substituents in the *para*-position of the 5-phenyl ring, while there appears to be greater room for substitution at the *meta*-position. (3) 2,6-Diubstitution of the pyridine ring cannot be accommodated sterically. These binding hypotheses are presently being tested through the evaluation of additional compounds. Furthermore, the modeling results presented herein are based mainly on steric complementarity. Several possible polar interactions between the enzyme and the crucial pyridine nitrogen of the inhibitors are suggested by the dockings. While a high degree of homology exists in the ATP binding pockets of ERK and CSBP (as with most kinases), differences do exist. Given the inability of the pyridinylimidazoles to inhibit ERK, selectivity most likely involves residues which are not conserved between ERK and CSBP. Consequently, in order to determine their importance, CSBP mutants in which active site residues (both polar and nonpolar) are altered are currently being constructed. The ability or inability of CSAID™ compounds to bind to these mutants should help determine the specific interactions that lead to the selectivity observed for the pyridinylimidazoles for CSBP.

Experimental

Biological assays

CSBP binding assay. The cytosolic fraction of the human monocytic cell line, THP.1, is incubated (~100 μg protein in 100 μL per tube) with 5 nM **II** and various concentrations of competitor, each diluted in 20 mM Tris-HCl pH 7.4, 20 mM Hepes buffer, and 1 mM $MgCl_2$ (binding buffer), for 15 min at rt. After incubation, the reaction mixtures (120 uL total volume) are chilled in an ice bath and separation of free from bound **II** is performed by size exclusion chromatography in a 4 °C cold room as follows. The reaction mixtures are applied to G-10 Sephadex straw columns (1.5 in bed volume) that were pre-equilibrated with 5 mL cold elution buffer (20 mM Tris-HCl pH 7.4 and 50 μM 2-ME). This is followed by another 400 μL addition of elution buffer, the eluent to this point being discarded. The bound ligand elutes in the protein-containing void volume with a final 500 uL elution, this 0.5 mL fraction being collected in 20 mL glass scintillation vials. After addition of 15 mL scintillation fluid, the vials are vortexed and the radioactivity accessed in a Beckman scintillation counter. Assay controls include binding of **II** to CSBP in the absence of competitor (Total Binding) and the lack of radioactivity measured in the absence of cytosol (Background). IC_{50}s are determined by linear regres-

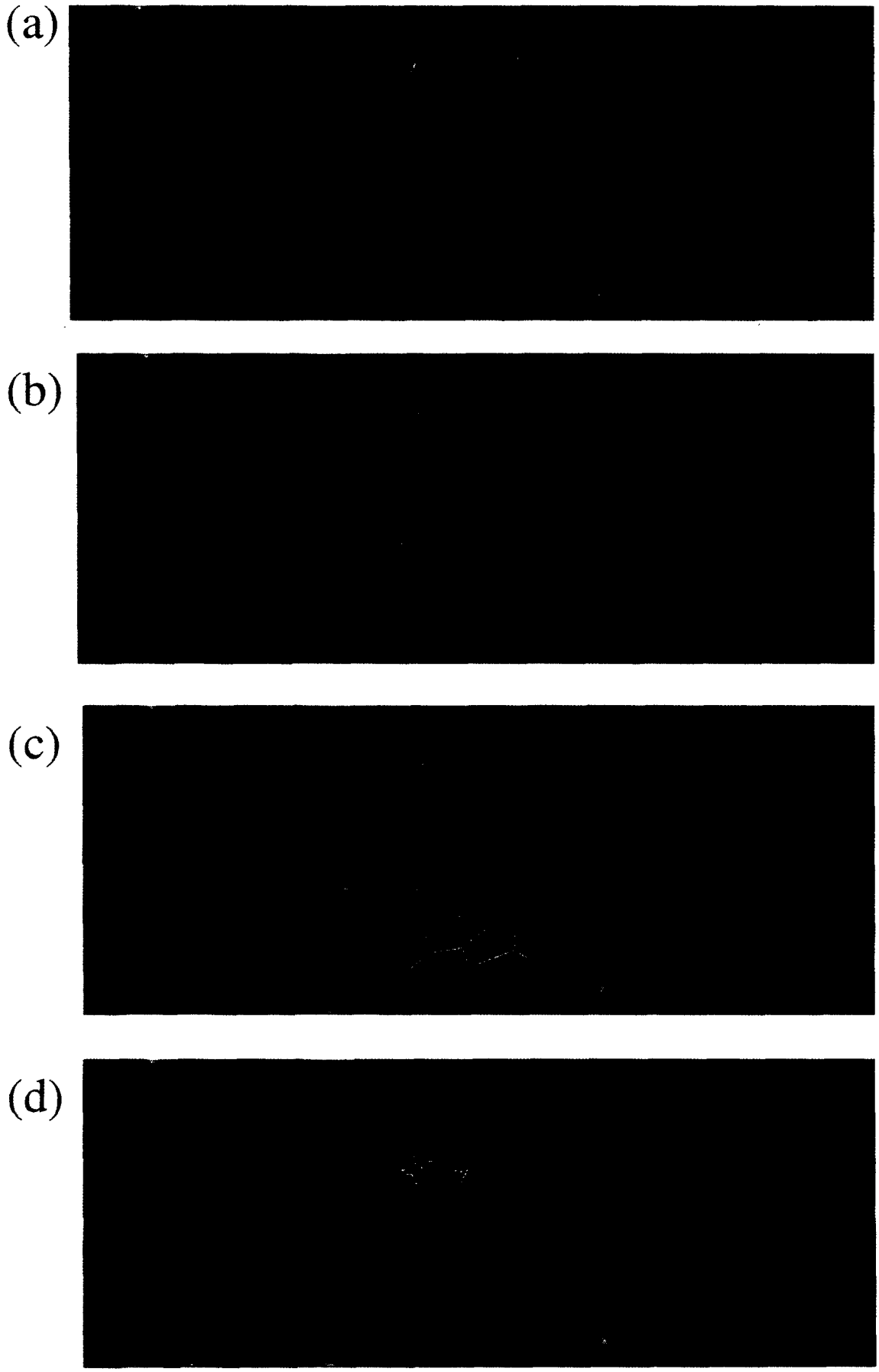

Figure 4. Proposed binding modes to CSBP. Connelly surfaces for both CSBP and SB 203580 were generated using Sybyl 6.22 (Tripos Corp.). (a) Binding of ATP based on ERK X-ray structure. (b) SB 203580 (**15**) bound in a mode in which the fluorophenyl ring interacts predominantly with residues in the top lobe of the ARP binding pocket. (c) SB 203580 bound in a mode in which the fluorophenyl ring binds primarily with residues in the bottom lobe of the ATP binding pocket. (d) SB 203580 bound in a mode in which the fluorophenyl and pyridyl rings interact with the top lobe of the ATP binding pocket.

sion analysis for a compound's ability to inhibit 50% of the radioligand binding to THP.1 cytosol/CSBP.

CSBP kinase assay. Mammalian CSBP2 was expressed with a $(His)_6$ tag in a HOG-1 deleted mutant of *S. cerevisiae* (kindly provided by M. M. McLaughlin and S. M. Fisher to be described elsewhere) and activated *in vivo* by osmotic shock. The enzyme was purified to >95% using Nickel chelate resin as previously described.[33] The kinase activity of purified CSBP2 was determined by measuring the incorporation of ^{32}P from γ-[^{32}P]ATP into an EGFR-derived peptide (T669) having the following sequence: KRELVEPLTPSGEAPNQALLR. Reactions (30 µL) contained 25 mM Hepes buffer, pH 7.4, 8 mM $MgCl_2$; 10 µM Na-vanadate; 1 mM EDTA, 0.8 µCi/170 µM 32P/ATP; 20 ng purified CSBP2; and 0.4 mM peptide. Compounds were incubated for 20 min at 4 °C with enzyme and peptide prior to adding ATP. Reactions were incubated for 10 min at 30 °C and were stopped by adding 10 µL of 0.3 M phosphoric acid. Phosphorylated peptide was isolated from the reaction mixture on phosphocellulose filter paper (p81). Filters were washed with 75 mM phosphoric acid and counted using a liquid scintillation counter.

ERK kinase assay. The ERK kinase assay was performed using a commercially available kit ($P44^{MPK}$, Upstate Biotechnology Inc.) with T699 peptide as the substrate and 0.4 ng of the purified kinase. Other incubation conditions were the same as for the CSBP kinase assay.

PKC kinase assay. The PKCα kinase assay was performed using the following modification of a published procedure:[34] The total volume in each well of a 96-well microtiter plate was 50 µL containing 10 mM Tris, pH 7.5; 1.1 m $CaCl_2$; 10 mM $MgCl_2$; 1.0 mM EGTA; 40 micrograms/mL phosphatidyl serine; 1 microgram/mL diolein; 100 micrograms/mL glycogen synthase peptide (Bachem Bioscience, Inc.) and 0.5 micrograms of partially purified protein kinase C. The reaction was initiated by the addition of 0.5 microcuries of γ-[^{32}P]ATP (6000 Ci/mmol, Amersham Life Science, Inc.) per well (approximately 10 micromolar final concentration) subsequent to addition of the various concentrations of test compounds. The reaction was stopped after 20 min at 37 °C by spotting 15 µL of the mixture onto a P30 filtermat (Wallac, Inc.). The filtermat was then washed extensively in 0.5% phosphoric acid, dried, and assayed for radioactivity by liquid scintillation spectrometry. The IC_{50} for PKC inhibition was determined using the following formula; [Log $IC_{50}=X_s+d(\Sigma x-0.5)$], where Σx represents the sum of the percent enzyme inhibition at each concentration, d is the log of the concentration drop per interval, and X_s is the log of the highest concentration tested.

PKA kinase assay. The PKA kinase was performed using the following modification of a published procedure:[35] The total volume in each well of a 96-well µL plate was 50 µL containing 50 mM MOPS pH 6.5, 20 mM $MgCl_2$, 10 µM Histone II-A, 2 uM cAMP and 0.5 micrograms of 3′:5′-cyclic AMP-dependent protein kinase (Sigma Chemical Company). The reaction was initiated by the addition of 0.5 microcuries of γ-[^{32}P]ATP (6000 Ci/mmol, Amersham Life Science, Inc.) per well (approximately 10 µM final concentration) subsequent to addition of the various concentrations of test compounds. Reactions were stopped after 20 min at 37 °C by spotting 15 µL of the mixture onto a P30 filtermat (Wallac, Inc.). The filtermat was then washed extensively in 0.5% phosphoric acid, dried and assayed for radioactivity by liquid scintillation spectrometry. The IC_{50} for PKA inhibition was determined using the following formula: [Log $IC_{50}=X_s+d(\Sigma x-0.5)$], where Σx represents the sum of the percent enzyme inhibition at each concentration, d is the log of the concentration drop per interval, and X_s is the log of the highest concentration tested.

Modeling

Homology model. The CSBP homology model was based on the 2.3 Å structure of the MAP kinase ERK2 by Zhang et al.[29] The sequences were aligned manually with consideration of the multiple sequence alignment of ERK2, cAPK, and Cdk2 presented in Zhang et al. Single residue insertions occurred at the end of strand Beta-3 (R57) and near the end of strand Beta-4 (T91). A six-residue deletion occurs in the activation loop after E178. The activation loop region from R173 to V183 was built using the backbone conformation from cAPK, which is the same length as the activation loop of CSBP. Since there are significant differences in the environment surrounding the activation loop in ERK2 compared with cAPK, we consider the activation loop conformation in this model to be speculative at best. Since the single-residue insertions were relatively distant form the ATP binding site, we did not attempt to build them in. Sidechains were built following the conformation of the existing sidechains in the ERK2 structure as much as possible. Global energy minimization was not used in order to avoid undue disruption of structure caused by a few bad contacts. The conformation of selected sidechains in regions of interest were adjusted manually.

Docking experiments. The Monte Carlo search algorithm in MacroModel V5.0[36] was employed for the generation of low energy conformers of SB 203580. The Amber force field and GB/SA water solvation model were used, and all conformers within a 50 kJ/mol window of the global minimum were saved.

Possible binding orientations for the inhibitor were generated using Dock 3.5[37] using both search and single modes. A region encompassing all residues within 10 Å of bound ATP was used for the generation of the protein surface to which ligands can be docked. In search mode, the single highest scoring docked orientation for each conformer was generated. In order to explore the possibility that lower scoring orientations may reflect the true binding mode, a search in

single mode was also carried out. In this case, a family of the highest scoring docked orientations were generated for a particular conformer of choice. The default values for INDOCK were employed except for mode (single or search) and bump_maximum (2).

Chemistry

General procedures. Melting points are uncorrected. IR spectra were recorded using KBR pellets. ^{1}H NMR spectra were recorded at 250 or 450 MHz. Unless otherwise noted, the NMR solvent was $CDCl_3$. MS were determined using the electrospray technique in the positive ion mode unless otherwise noted. When air- or moisture-sensitive reagents were used, reactions were run under argon. THF was dried by distillation from sodium and benzophenone. Aldrich 'gold label' toluene and CH_2Cl_2 were used if it was necessary for these solvents to be dry. Chromatography refers to purification by flash chromatography on E. Merck silica gel 60 (230–400 mesh).

General procedure[38] for the preparation of N-1-substituted 4,5-diarylimidazoles—Scheme 2

1-[3-(4-Morpholinyl)propyl]-4-(4-fluorophenyl)-5-(4-pyridyl)imidazole (5). A solution of 4-fluorobenzaldehyde (13.1 mL, 122 mmol), thiocresol (16.64 g, 122 mmol), formamide (15.0 mL, 445 mmol), and toluene (300 mL) were combined and heated to reflux with azeotropic removal of H_2O for 18 h, cooled, diluted with EtOAc (500 mL) and washed with satd aq Na_2CO_3 (3 × 100 mL), brine (100 mL), dried (Na_2SO_4) and concentrated. The residue was triturated with petroleum ether, filtered and dried in vacuo to afford 28.50 g (85%) of 4-fluorophenyl-tolylthiomethylformamide as a white solid: m.p. 119–120 °C; ^{1}H NMR: δ 8.03 (s, 1H), 7.71 (d, 2H), 7.48 (m, 2H), 7.36 (d, 2H), 7.11 (t, 2H), 6.30 (s, 1H), 2.46 (s, 3H).

To a stirred solution of 4-fluorophenyl-tolylthiomethylformamide (25 g, 91 mmol) in CH_2Cl_2 (300 mL) at −30 °C was added dropwise $POCl_3$ (11 mL, 110 mmol) followed by the dropwise addition of Et_3N (45 mL, 320 mmol). The reaction mixture was stirred at −30 °C for 30 min and 5 °C for 2 h, diluted with CH_2Cl_2 (300 mL) and washed with 5% aq Na_2CO_3 (3 × 100 mL), dried (Na_2SO_4) and concentrated to 500 mL. The resulting solution was filtered through 2 L of silica in a large sintered glass funnel with CH_2Cl_2 to afford 12.5 g (53%) of 4-fluorophenyl-tolylthiomethylisocyanide as a light brown, waxy solid: IR (CH_2Cl_2): 2130 cm^{-1}; ^{1}H NMR: δ 7.39 (d, 2H), 7.25 (m, 2H), 7.19 (d, 2H), 7.10 (t, 2H), 5.76 (s, 1H), 2.37 (s, 3H).

Pyridine-4-carboxaldehyde (2.14 g, 20 mmoL), 4-(3-aminopropyl)morpholine (2.88 g, 20 mmol), toluene (50 mL) and $MgSO_4$ (2 g) were combined and stirred for 18 h. The reaction mixture was filtered and the filtrate was concentrated to afford pyridine-4-carboxaldehyde [4-morpholinylprop-3-yl]imine (4.52 g, 97%) as a yellow oil containing less than 5% of aldehyde based on ^{1}H NMR: δ 8.69 (d, 2H), 8.28 (s, 1H), 7.58 (d, 2H), 3.84 (m, 6H), 2.44 (m, 6H), 1.91 (m, 2H).

To a solution of 4-fluorophenyl-tolylthiomethylisocyanide (1.41 g, 5.5 mmol), pyridine-4-carboxaldehyde [4-morpholinylprop-3-yl]imine (1.17 g, 5.0 mmol) and CH_2Cl_2 (10 mL) at 5 °C was added 1.5.7-triazabicyclo-[4.4.0]dec-5-ene (TBD; 0.71 g, 5.0 mmol). The reaction was kept at 5 °C for 16 h, diluted with EtOAc (80 mL) and washed with satd aq Na_2CO_3 (2 × 15 mL). The organic phase was extracted with 1 N HCl (3 × 15 mL), and the combined acid phases were washed with EtOAc (2 × 25 mL), layered with EtOAc (25 mL) and made basic by the addition of solid K_2CO_3 until pH 8.0 and then 10% NaOH until pH 10. The phases were separated and the aqueous phase was extracted with additional EtOAc (3 × 25 mL). The combined extracts were dried (K_2CO_3), concentrated and the residue was crystallized from acetone/hexane to afford 0.94 g (51%) of **5**: m.p. 149–150 °C; Anal. calcd for $C_{21}H_{23}FN_4O \cdot 1/4H_2O$: C, 68.00; H, 4.79; N, 13.31. Found: C, 64.86; H, 4.67; N, 13.15%.

Preparation 2,4,5-triarylimidazoles—Scheme 1: General procedure for method A

4-(4-Fluorophenyl)2-(4-methylsulfinylphenyl)-5-(4-pyridyl)-1*H*-imidazole (7). To a solution of 4-pyridylcarbinol (1520 g, 13.9 mol) and imidazole (1897 g, 27.9 mol) in DMF (4.2 L) at 5 °C was added *tert*-butyldimethyl-silylchloride (2100 g, 13.9 mol) at such a rate that the temperature did not rise above 5 °C. Upon completion of addition, the ice bath was removed and the reaction was stirred at ambient temperature for 18 h. The reaction mixture was poured into ice–H_2O (9.5 L), and extracted with EtOAc (3 × 4L). The combined extracts were washed with H_2O (3 × 6L), dried (Na_2SO_4) and concentrated in vacuo to afford 4-(*tert*-butyldimethylsiloxy)methyl pyridine (3016 g, 97%) suitable for use in the following step: ^{1}H NMR: δ 8.55 (d, 2H); 7.24 (d, 2H); 4.72 (s, 2H); 0.91 (s, 9H); 0.09 (s, 6H).

To a solution of diisopropylamine (64.4 mL, 0.46 mol) and THF (120 mL) at −20 °C was added *n*-butyllithium (207.8 mL, 0.52 mol, 2.5 M solutions in hexanes) dropwise over 15 min. After stirring at this temperature for 0.5 h, 4-(*tert*-butyldimethylsilyoxy)-methyl pyridine (98.14 g, 0.44 mol) was added dropwise over 20 min. Stirring was continued at −20 °C for 45 min and a solution of 4-fluoro-*N*-methoxy-*N*-methylbenzamide (84.5 g, 0.46 mol) in THF (90 mL) was added dropwise over 0.5 h. Once addition was complete, the reaction mixture was warmed to 0 °C for 1 h and stirred at ambient temperature for 1.5 h. The mixture was poured into a solution of satd aq NH_4Cl (98 g) and H_2O (500 mL) and extracted with EtOAc (3 × 250 mL). The combined organic extracts were washed with H_2O, brine, and dried ($MgSO_4$). Evaporation of the solvent in vacuo afforded 2-(*tert*-butyldimethylsilyloxy)-1-(4-fluorophenyl)-2-(4-pyridyl)ethanone as an amber oil; yield 114.2 g (75%).

A mixture of NH_4OAc (402 g, 5.2 mol) and $Cu(OAc)_2 \cdot H_2O$ (26 g, 0.14 mol) in AcOH (780 mL) was heated to 100 °C and a solution of 2-(*tert*-butyldimethylsilyloxy)-1-(4-fluorophenyl)-2-(4-pyridyl)ethanone (180 g, 0.52 mol) and 4-(methyl-thio)benzaldehyde (87 g, 0.57 mol) in AcOH (520 mL) was added dropwise at 98 °C over 40 min. The reaction mixture was heated for an additional 40 min at 98 °C cooled rapidly and poured into a mixture of ice (2.8 Kg), concd aq NH_4OH (4,2 L) and EtOAc (2.8 L). After stirring for ~15 min, the layers were separated and the aqueous phase extracted with EtOAc (2 × 1.75 L). The combined organic extracts were washed with H_2O (3 × 6 L), brine and dried ($MgSO_4$). The solvent was eavaporated in vacuo and the residue was added to acetone (900 mL) and heated on a steam bath. The resulting slurry was cooled in an ice bath and the solids were collected and washed sparingly with ether to afford chromatographically pure (5% MeOH in CH_2Cl_2) 4-(4-fluorophenyl)2-(4-methylthiophenyl)-5-(4-pyridyl)-1*H*-imidazole (**43**); 83 g (44%). An analytically pure sample was obtained by recrystallization from MeOH: m.p. 239–240; ^{1}H NMR: δ 9.97 (br s, 1H); 8.48 (d, 2H); 8.84 (d, 2H); 7.54 (d, 2H); 7.43 (q, 2H); 7.32 (d, 2H); 7.19 (q, 2H); MS: *m/z* 362 ($M^+ + H$); Anal. calcd for $C_{21}H_{16}FN_3S$: C, 69.78; H, 4.46; N, 11.63. Found: C, 69.76; H, 4.42; N, 11.65%.

To a solution of **43** (0.80 g, 2.2 mmol) in AcOH (30 mL) was added a solution of $K_2S_2O_8$ (0.72 g, 2.6 mmol) in H_2O (20 mL). After stirring for 18 h, the reaction mixture was poured into H_2O and neutralized by the addition of concd NH_4OH. The resulting precipitate was collected to afford chromatographically pure (4% MeOH in CH_2Cl_2) **7** as a tan solid; yield 0.65 g (78%). An analytically pure white solid could be obtained by recrystallization from MeOH: m.p. 250–252 °C, ^{1}H NMR ($CDCl_3$/MeOH-d_4): δ 8.37 (d, 2H); 8.13 (d, 2H); 7.64 (d, 2H); 7.45 (m, 4H); 7.07 (m, 2H); 2.74 (s, 3H); MS: *m/z* 378 ($M^+ + H$); Anal. calcd for $C_{21}H_{16}FN_3OS$: C, 66.83; H, 4.27; N, 11.13. Found: C, 66.79; H, 4.35; N, 11.14%.

General procedure for method B

2-(4-Aminomethylphenyl)-4-(4-fluorophenyl)-5-(4-pyridyl)-1*H*-imidazole (51). To a mixture containing methoxymethylamine hydrochloride (44 g, 0.45 mol) and triethylamine (138 mL, 0.99 mol) in CH_2Cl_2 (500 mL) at 0 °C was added 4-fluorobenzoyl chloride (50 mL, 0.41 mol) over 30 min. The ice-bath was removed and after stirring for an additional 30 min, the reaction mixture was poured into H_2O and extracted with EtOAc. The organic extract was washed with brine and dried ($MgSO_4$). Removal of the solvent in vacuo afforded 4-fluoro-*N*- methoxy-*N*-methylbenzamide (80 g, 100%) which was used without further purification: ^{1}H NMR: δ 7.72 (dd, 2H); 7.06 (t, 2H); 3.52 (s, 3H); 3.43 (s, 3H).

To a solution of diisopropylamine (21 mL, 0.15 mol) in THF (250 mL) at −78 °C was added *n*-butyllithium (54 mL of a 2.5 M solution in hexanes, 0.135 mol). after stirring for 15 min, 4-picoline (10 g, 0.108 mol) was added and the reaction mixture was stirred for an additional 15 min at −78 °C after which time 4-fluoro-*N*-methoxy-*N*-methylbenzamide (20 g, 0.109 mol) was added. The reaction was allowed to warm slowly to ambient temperature, poured into brine and extracted with THF:CH_2Cl_2 4:1. The organic extract was dried ($MgSO_4$) and the solvent was removed in vacuo. Recrystallization of the residue from Et_2O/hexanes afforded 1-(4-fluorophenyl)-2-(4-pyridyl)ethanone as an off-white solid suitable for use in the next step; yield 16.8 g (72%): ^{1}H NMR: δ 8.55 (d, 2H); 8.03 (dd, 2H); 7.16 (m, 4H); 4.24 (s, 2H).

To a solution of 1-(4-fluorophenyl)-2-(4-pyridyl)ethanone (16.5 g, 0.077 mol) in 3 N HCl (250 mL) at ambient temperature was added a solution of $NaNO_2$ (6.3 g, 0.092 mol) in H_2O (250 mL). After stirring at ambient temperature for 0.5 h, the reaction mixture was neutralized by the addition of 50% aq NaOH. The resulting precipitate was collected, washed with H_2O, acetone and dried in vacuo to afford chromatographically pure (4% MeOH in CH_2Cl_2) 1-(4-fluorophenyl)-2-hydroxyimino-2-(4-pyridyl)ethanone as a tan solid; yield 14 g (74%): MS: *m/z* 245 ($M^+ + H$).

To a solution of 1-(4-fluorophenyl)-2-hydroxyimino-2-(4-pyridyl)ethanone (10 g, 0.041 mol) and 4-cyanobenzaldehyde (8.0 g, 0.061 mol) in AcOH (150 mL) was added NH_4OAc (20 g, 0.26 mol). After heating to reflux for 18 h, the reaction mixture was poured into H_2O and neutralized with concd NH_4OH. The resulting precipitate was collected, washed with water, air dried and triturated with ether to afford 2-(4-cyanophenyl)-4-(fluorophenyl)-*N*-1-hydroxy-5-(4-pyridyl)imidazole as an off-white solid in quantitative yield: ^{1}H NMR: δ 8.27 (d, 2H); 7.94 (d, 2H); 7.72 (d, 2H); 7.35 (d, 2H); 7.30 (dd, 2H); 6.96 (t, 2H).

To a solution of 2-(4-cyanophenyl)-4-(fluorophenyl)-*N*-1-hydroxy-5-(4-pyridyl)imidazole (4.5 g, 1.32 mmol) in DMF (50 mL) was added triethyl-phosphite (3.4 mL, 20 mmol). The reaction mixture was heated to 100 °C for 2 h, cooled to ambient temperature and poured into H_2O. The resulting precipitate was collected, washed with H_2O and dried in vacuo to afford 2-(4-cyanophenyl)-4-(fluorophenyl)-5-(4-pyridyl)-1*H*-imidazole as a white solid; yield 4.0 g, 89%). An analytical sample was obtained by recrystallization from CH_2Cl_2/MeOH: m.p. 268–269 °C; ^{1}H NMR ($CDCl_3$/MeOH-d_4): δ 8.35 (br, s, 2H), 8.04 (d, 2H), 7.67 (d, 2H), 7.41 (br m, 5H), 7.06 (br m, 2H); MS (DCI/NH_3): *m/z* 341 ($M^+ + H$); Anal. calcd for $C_2H_{13}FN_4$: C, 74.11; H, 3.85; N, 16.46. Found: C, 73.70; H, 3.69; N, 16.37%.

To a solution of 2-(4-cyanophenyl)-4-(fluorophenyl)-5-(4-pyridyl)-1*H*-imidazole (2.5 g, 7.3 mmol) in THF was added $LiAlH_4$ (11.3 mL of a 1 M solution in THF, 11.3 mmol). The reaction mixture was heated to reflux for 2.5 h, cooled to ambient temperature and poured into 2.5 N NaOH. The resulting mixture was extracted with THF and the organic extract was washed with brine and concentrated under reduced pressure. The residue was chromatographed successively with $CHCl_3$:MeOH 9:1 and $CHCl_3$:MeOH:concd NH_4OH

90:10:1. Fractions containing only the major component were combined and the solvent was removed in vacuo. The residue was triturated with Et_2O to afford **51** as an off-white solid; yield 1.5 g (60%). An analytical sample was obtained by recrystallization from 2-propanol: m.p. 214–215 °C; ^{1}H NMR: δ 8.50 (br s, 2H), 8.02 (d, 2H), 7.61 (appt. t, 2H), 7.48 (m, 4H), 7.34 (br s, 3H), 3.80 (s, 2H); MS: *m/z* 345 ($M^+ + H$); Anal. calcd for $C_{21}H_{17}FN_4 \cdot 1/3H_2O$: C, 72.29; H, 5.06; N, 16.06. Found: C, 72.18; H, 5.18; N, 15.56%.

General procedure for the preparation of 2,3-diarylpyrroloimidazoles—Scheme 3

2-(4-Methylsulfinylphenyl)-3-(4-pyridyl)-6,7-dihydro-[5*H*]-pyrrolo[1,2-*a*]imidazole (SK&F 105809, 28). To a solution of 2-chloro-4′-fluoroacetophenone (104 g, 0.063 mol) in $CHCl_3$ (950 mL) at 1 °C was added 2-iminopyrrolidine[39] (59 g, 0.702 mol) over a 10 min period with mechanical stirring and keeping the temperature between 1 and 4 °C. The cooling bath was removed and the reaction was stirred at ambient temperature for 3 h. The resulting suspension was poured into EtOAc (1 L) and the solids were collected, washed with EtOAc (500 mL) and dried in vacuo at 35 °C to afford 116 g (75%) of 2-(2-iminopyrrolidin-1-yl)-4′-fluoroacetophenone hydrochloride. An analytically pure sample was obtained by recrystallization from EtOH: m.p. 207–208 °C; Anal. calcd for $C_{12}H_{14}ClFN_2O$: C, 56.15; H, 5.50; N, 10.91. Found: C, 56.14; H, 5.50; N, 10.90%.

A solution of 2-(2-iminopyrrolidin-1-yl)-4′-fluoroacetophenone hydrochloride (112 g, 0.436 mol) in H_2O (1.1 L) was heated to reflux for 9 h. After cooling to 25 °C, the reaction mixture was filtered and the pH of the filtrate was adjusted to 6.5 by the addition of solid $NaHCO_3$. The resulting precipitate was collected, washed with H_2O and dried at 50 °C in vacuo to give 64 g (77%) of 2-(4-fluorophenyl)-6,7-dihydro-[5*H*]-(1,2-*a*)imidazole: An analytically pure sample was obtained by recrystallization from CCl_4: m.p. 137.5–139 °C; Anal. calcd for $C_{12}H_{11}FN_2$: C, 71.27; H, 5.48; N, 13.85. Found: C, 71.00; H, 5.61; N, 13.73%.

To a mechanically stirred solution of 2-(4-fluorophenyl)-6,7-dihydro-[5*H*]-(1,2-*a*)imidazole (66.5 g, 0.348 mol) and pyridine (267 mL, 3.3 mol) in CH_2Cl_2 at 5 °C was added ethyl chloroformate (267 mL, 1.7 mol) over 0.5 h, keeping the internal temperature between 5 and 10 °C. The ice bath was removed and the reaction was stirred at ambient temperature for 8 to 16 h. The reaction was cooled to 5 °C and 267 mL of pyridine was added in one portion followed by the dropwise addition of ethyl chloroformate over 1 h, keeping the internal temperature between 5 and 10 °C. The ice bath was removed and the reaction was stirred at ambient temperature for 6 to 10 h. The sequential addition of pyridine and ethyl chloroformate and subsequent stirring was repeated two more times. The solvent was removed in vacuo and the residue was dissolved in CH_2Cl_2 and washed with 1.0 N HCl (2 × 1 L). The organic phase was washed with 10% aq K_2CO_3, dried (K_2CO_3) and filtered. The filrate was evaporated and the residue was triturated with 250 mL of warm toluene (50 °C) and cooled to 5 °C. The resulting precipitate was collected, washed with 100 mL of toluene and dried at 40 °C in vacuo to give 92.2 g (75%) of 3-[1-ethoxycarbonyl-(1,4-dihydropyridyl)]-2-(4-fluorophenyl)-6,7-dihydro-[5*H*]-pyrrolo-(1,2-*a*)imidazole: m.p. 146–147 °C.

Oxygen was bubbled at a moderate rate for 5 min into a solution of *tert*-butanol (4.2 L) and potassium *tert*-butoxide (266 g, 2.4 mol). 3-[1-Ethoxycarbonyl-(1,4-dihydropyridyl)]-2-(4-fluorophenyl)-6,7-dihydro-[5*H*]-pyrrolo-[1,2-*a*]imidazole (420 g, 1.19 mol) was added in one portion and the reaction mixture was heated to reflux for 3 h using a slow oxygen purge. The reaction was cooled below reflux. Additional potassium *tert*-butoxide (134 g) was added and the reaction mixture was heated to reflux for 16 h. The reaction was cooled to 50 °C and toluene (4 L) was added. The solvent was evaporated in vacuo and the residue was partitioned between CH_2Cl_2 (6 L) and 5% aq Na_2CO_3 (3 L). The layers were separated and the aqueous layer was extracted with 2 × 2 L of CH_2Cl_2. The combined organic extracts were dried (Na_2CO_3), filtered and the filtrate concentrated in vacuo to give an oil. Toluene (4 L) was added to the residue and evaporated to give a thick slurry which solidified upon cooling to 25 °C. The solid was collected, washed with toluene (100 mL) and dried at 50 °C to give 133 g (40%) of 2-(4-fluorophenyl)-3-(4-pyridyl)-6,7-dihydro-[5*H*]-pyrrolo[1,2-*a*]imidazole (**9**): m.p. 165–166 °C; Anal. calcd for $C_{17}H_{14}FN_3$: C, 73.10; H, 5.05; N, 15.04. Found: C, 73.31; H, 5.11; N, 15.08%. An additional 46 g (14%) of **9** was obtained by concentrating the filtrate and triturating the residue with ethyl acetate (300 mL).

To a solution of **9** (270 g, 0.968 mol) in DMF (3.7 L) was added sodium thiomethoxide (81.0 g, 1.16 mol) with mechanical stirring at 25 °C. The reaction mixture was heated to 80 °C for 18 h, cooled to 25 °C and poured into H_2O (11 L) at 5 °C. The resulting precipitate was collected and washed with H_2O (3 × 2 L) and dried in vacuo at 60 °C to give 218 g (73%) of 2-(4-methylthiophenyl)-3-(4-pyridyl)-6,7-dihydro-[5*H*]-pyrrolo[1,2-*a*]-imidazole (**26**). An analytical sample was obtained by recrystallization from EtOAc: m.p. 171–172 °C; ^{1}H NMR: δ 8.58 (d, 2H), 7.46 (d, 2H), 7.25 (d, 2H), 7.18 (d, 2H), 4.04 (t, 2H), 2.68 (m, 2H), 2.50 (s, 3H). Anal. calcd for $C_{18}H_{17}N_3S$: C, 70.33; H, 5.57; N, 13.67; S, 10.43. Found: C, 69.93; H, 5.40; N, 13.76; S, 10.75%.

To a solution of **26** (168 g, 0.547 mol) in H_2O (1.7 L) and aq HCl (907 mL of a 1.2 N solution, 1.09 mol) at 5 °C was added sodium periodate (105 g, 0.491 mol) in 1.7 L of H_2O over a 3 h period, keeping the internal temperature between 5 and 6 °C. After stirring for 18 h a 5 °C, the reaction was warmed to 20 °C and the pH adjusted to 3.6 with 10% aq Na_2CO_3. The aqueous solution was washed with CH_2Cl_2 (4 × 1 L). Norit A (30 g) was added to the aqueous phase and the mixture was stirred for 0.5 h. The solids were removed by filtration and the pH of the filtrate was adjusted to 10 with Na_2CO_3 and

extracted with CH_2Cl_2 (6 × 1 L). The organic extracts were combined, dried (Na_2CO_3) and concentrated to give a viscous gum which crystallized upon trituration with boiling EtOAc (550 mL). The suspension was cooled to 25 °C, filtered and the solids were washed with EtOAc (100 mL) and dried in vacuo at 40 °C to afford 106 g (60%) of **28**: m.p. 163.5–165.5 °C; ^{1}H NMR (360 MHz): δ 8.62 (2H, d), 7.68 (2H, d), 7.68 (2H, d), 7.57 (2H, d), 7.25 (2H, d), 4.05 (2H, t), 3.02 (2H, t), 2.72 (s) superimposed upon 2.69 (5H, m); MS (DCI): *m/z* 324 ($M^+ + H$). An analytically pure sample was obtained by recrystallization from EtOAc: Anal. calcd for $C_{18}H_{17}N_3OS$: C, 66.85; H, 5.30; N, 12.99. Found: C, 67.02; H, 5.370; N, 13.03%.

Acknowledgments

We would like to acknowledge Megan M. McLaughlin, Seth M. Fisher, Terry G. Porter, and George Levi for generating acvtive CSBP2. We would like to express our gratitude to Professor Elizabeth J. Goldsmith for providing us with the ERK coordinates. We would also like to thank Edith Reich for performing the microanalyses.

References

1. For a series of recent reviews on signal transduction see: *Cell* **1995**, *80*, 179.

2. Hunter, T. *Enzymology (Protein Kinase Clasification)*; Hunter, T.; Sefton, B. M., eds.; Academic Press; San Diego, 1991; Vol. 200, p. 3.

3. For reviews specifically addressing signal transduction involving MAP kinases see: Marshall, C. J. *Cell* **1995**, *80*, 179; Herskowitz, I. *Cell* **1995**, *80*, 187; Hunter, T. *Cell* **1995**, *80*, 225.

4. Weinstein, S. L.; Jurne, C. H.; DeFranco, A. L. *J. Immunol.* **1993**, *151*, 3829.

5. Han, J.; Lee, J. D.; Bibbs, L.; Ulevitch, R. J. *Science* **1994**, *265*, 808.

6. Lee, J. C.; Griswold, D. E.; Votta, B.; Hanna, N. *Int. Immunopharmacol.* **1988**, *10(7)*, 835.

7. Lee, J. C.; Badger, A. M.; Griswold, D. E.; Dunnington, D.; Truneh, A.; Votta, B.; White, J. R.; Young, P. R.; Bender, P. E. *Ann. N.Y. Acad. Sci.* **1993**, *696*, 149.

8. Young, P. R.; McDonnell, P.; Dunnington, D.; Hand, A.; Laydon, J.; Lee, J. C. *Agents Actions* **1993**, *39*, C67.

9. Prichett, W.; Hand., A.; Sheilds, J.; Dunnington, D. *J. Inflamm.* **1995**, *45*, 97.

10. Gallagher, T. F.; Fier-Thompson, S. M.; Garigipati, R. S.; Sorenson, M. E.; Smietana, J. M.; Lee, D.; Lee, J. C.; Laydon, J. T.; Griswold, D. E.; Chabot-Fletcher, M. C.; Breton, J. J.; Adams, J. L. *Bioorg. Med. Chem. Lett.* **1995**, *5*, 1171.

11. Brewster, J. L.; de Valoir, T.; Dwyer, N. D.; Winter, E.; Gustin, M. C. *Science* **1993**, *259*, 1760.

12. Lee, J. C.; Laydon, J. T.; McDonnell, P. C.; Gallagher, T. F.; Kumar, S.; Green, D.; McNulty, D.; Blumenthal, M. J.; Heys, J. R.; Landvatter, S. W.; Strickler, J. E.; McLaughlin, M. M.; Siemens, I. R.; Fisher, S. M.; Livi, G. P.; White, J. R.; Adams, J. L.; Young, P. R. *Nature* **1994**, *372*, 739.

13. Han, J.; Richter, B.; Liu, Z.; Kravchenko, V. V.; Ulevitch, R. J. *Biochim. Biophys. Acta* **1995**, *1265*, 224.

14. Lin, A.; Minden, A.; Martinetto, H.; Claret, F.-S.; Lange-Carter, C.; Mercurio, F.; Johnson, G. L.; Karin, M. *Science* **1995**, *268*, 286.

15. Derijard, B.; Raingeaud, J.; Barret, T.; Wu, I.-H.; Han, J.; Ulevitch, R. Jl; Davis, R. J. *Science* **1995**, *267*, 682.

16. Raingeaud, J.; Witmarsh, A. J.; Barrett, T.; Derijard, B.; Davis, R. *J. Mol. Cell Biol.* **1996**, *16(3)*, 1247.

17. Han, J. H.; Lee, J. D.; Jiang, Y.; Li, Z. G.; Feng, L. L.; Ulevitch, R. J. *J. Biol. Chem.* **1996**, *271(6)*, 2886.

18. Cuenda, A.; Rouse, J.; Doza, Y. N.; Meier, R.; Cohen, P.; Gallagher, T. F.; Young, P. K.; Lee, J. C. *FEBS Lett.* **1995**, *264*, 229.

19. McLaughlin, M. M.; Kumar, S.; McDonnell, P. C.; Van Horn, S.; Lee, J. C.; Livi, G. P.; Young, P. R. *J. Biol. Chem.* **1996**, *271*, 8488.

20. Kaspar, R. L.; Gehre, L. *J. Immunol.* **1994**, *153*, 277.

21. Kruys, V.; Beutler, B.; Huez, G. *Enzyme* **1990**, *44*, 193.

22. Beutler, B.; Han, J.; Kreus, V.; Giroir, B. P.; *Tumor Necrosis Factors: The Molecules and Their Emerging Role in Medicine*; Beutler, B., Ed.; Raven Press, Ltd: New York, 1992, pp 561–574.

23. For a discussion of translational repression and its role in the regulation of cytokine biosynthesis see: Lee, J. C.; Young, P. R. *J. Leuk. Biol.* **1996**, *59*, 1, and therein.

24. For a review on the potential therapeutic utility of antagonizing cytokine action or inhibiting cytokine production see: Henderson, B.; Blake, S. *TiPS* **1992**, *13*, 145.

25. Lee, J. C.; Votta, B.; Dalton, B. J.; Griswold, D. E.; Bender, P. E.; Hanna, N. *Int. J. Immunother.* **1990**, *VI(1)*, 1.

26. Lee et al. have previously published a correlation between CSBP binding and in vitro IL-1 inhibition and has shown a correlation coefficient of 0.9: see ref 12.

27. Lantos, I.; Gombatz, K.; McGuire, M.; Pridgen, L.; Remich, J.; Shilcrat, S. *J. Org. Chem.* **1988**, *53*, 4223.

28. Lantos, I.; Bender, P. E.; Razgaitis, K. A.; Sutton, B. M.; DiMartino, M. J.; Griswold, D. E.; Walz, D. T. *J. Med. Chem.* **1984**, *27*, 72.

29. Zhang, F.; Strand,. A.; Robbins, D.; Cobb, M. H.; Goldsmith, E. J. *Nature* **1994**, *367*, 704.

30. Kassis, S. Personal communication.

31. Kumar, S. Personal communication.

32. Zheng, J.; Knighton, D. R.; Xuong, N.-H.; Taylor, S. S.; Sowadski, J. M.; Eyck, L. F. *Protein Sci.* **12993**, *2*, 1559.

33. Kumar, S.; McLaughlin, M. M.; McDonnell, P. C.; Lee, J. C.; Livi, G. P.; Young, P. R. *J. Biol. Chenm.* **1996**, *270*, 29043.

34. Castagna, M.; Takai, Y.; Kaibuchi, K.; Sano, K; Kikkawa, U.; Nishizuka, Y. *J. Biol. Chem.* **1982**, *267*, 7847.

35. Murray, K. J.; England, P. J.; Lynham, J. A.; Mills, D.; Schmitz-Peiffer, C.; Reeves, M. L. *Biochem. J.* **1990**, *267*, 703.

36. Still, W. C. MacroModel V5.0, Columbia University, New York, NY, 1995.

37. Kuntz, I. D. Dock 3.5. University of San Francisco, San Francisco, CA, 1995.

38. For further experimental procedures for compounds in this series see: Boehm, J. C.; Smietana, J. M.; Sorenson, M. E.; Garigipati, R. S.; Gallagher, T. F.; Sheldrake, P. L.; Bradbeer, J.; Badger, A. M.; Laydon, J. T.; Lee, J. C.; Hillegass, L. M.; Griswold, D. E.; Breton, J. J.; Chatbot-Fletcher, M. C.; Adams, J. L. *J. Med. Chem.* **1996**, *39*, 3929.

39. Moriconi, E. J.; Cevasco, A. A. *J. Org. Chem.* **1968**, *33*, 2109.

(*Received in U.S.A.* 26 *April* 1996; *accepted* 5 *June* 1996)